Physical-Layer Network Coded QAM with Trellis Shaping for the Two-Way Relay Channel

Daniela Donati and Mark F. Flanagan
School of Electrical and Electronic Engineering
University College Dublin
Dublin, Ireland
Email: daniela.donati@ucdconnect.ie, mark.flanagan@ieee.org

***Abstract*—Physical-layer network coding (PNC) allows to improve the throughput on the two-way relay channel (TWRC). PNC systems using higher-order modulation present some challenges regarding how to design the PNC mapping at the relay. With higher-order modulation it is also desirable to use constellation shaping which allows to minimize the average transmitted energy. In this paper, we show how low-complexity trellis shaping can be used to provide constellation shaping both at the user nodes *and* at the relay node. The proposed technique works specifically for sign bit shaping and M-ary quadrature amplitude modulation (QAM). Simulation results show that the proposed scheme provides a significantly increased performance in terms of the achievable BER, with 5.3dB shaping gain available at a BER of 10^{-3} in the case of 256-QAM signaling.**

I. Introduction

In a two-way relay channel (TWRC), a *relay node* allows a pair of *user nodes* to exchange information when no direct link exists between the user nodes. The number of time slots required to complete a communication depends on how the information is processed at the relay [1]. Using physical-layer network coding (PNC) [2], the required number of time slots is two. The transmission schedule for PNC is depicted in Fig. 1. PNC requires two fewer time slots compared to sequential relaying and one fewer time slot compared to traditional network coding [1]. In the first time slot, called the *multiple access* (MA) phase, both users transmit information to the relay simultaneously. The relay receives the superposition of the users' signals, and broadcasts a network-coded signal in the second slot; this is called the *broadcast* (BC) phase. The network-coded signal is a function of the superimposed signal received at the relay. In [2] the concept of PNC was originally proposed for the scenario of binary modulation, where the superimposed signal is mapped to a network-coded signal representing an exclusive-OR (XOR) of the users' bits. Bitwise XOR mapping however causes ambiguity issues in systems with higher-order modulation, which are required for high-data-rate applications. In [3] the superimposed signal is mapped to a codeword in order to avoid ambiguity in a binary modulation scenario. In [4], PNC with higher-order pulse amplitude modulation (PAM) is considered and optimal symbol and bit mappings for uniform and non-uniform PAM are presented. This optimal mapping ensures network coding is ambiguity-free and provides improved bit error rate (BER) performance. In [5] a constellation mapping for PNC with M-ary quadrature amplitude modulation (QAM) was proposed.

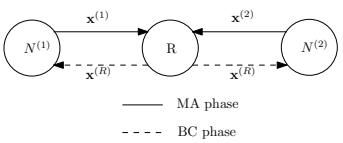

Figure 1. Physical-layer network coding scheme. $N^{(i)}, i \in \{1, 2\}$ are the user nodes, while R is the relay node. $\mathbf{x}^{(i)}$ and $\mathbf{x}^{(R)}$ are the transmitted signals in the MA phase and the BC phase respectively.

Constellation shaping, proposed in [6], allows to minimize the average transmitted energy for a fixed minimum Euclidean distance constellation. In practice, constellation shaping is implemented using a *shaping code* which will select more frequently those constellation points having lower energy. In [7] it was shown that for PNC systems, the achievable shaping gain is much higher than that for the point-to-point Gaussian channel. The authors of [7] also proposed a system which combines PNC with higher-order PAM and constellation shaping. The method, which achieved a substantial shaping gain, used a block shaping code which was designed to avoid ambiguity in the relay mapping; however, the shaping decoding complexity was exponential in the input word length of the block shaping code.

In this paper, a shaped PNC system using M-ary QAM is proposed, based on implementation of *trellis shaping* [8] both at the user nodes *and* at the relay. Trellis shaping reduces the complexity of the system compared to block shaping codes. We will demonstrate that the proposed approach is effective in increasing the energy efficiency of the system for a range of QAM constellation sizes.

The paper is organized as follows. Section II provides an overview of the trellis shaping technique and its implementation. In Section III, the application of trellis shaping to the PNC system is presented, while in Section IV presents the obtained simulation results for the proposed system. Section V provides concluding remarks.

II. Trellis Shaping Overview

Trellis shaping, presented in [8], is an efficient and low-complexity method for achieving constellation shaping. In this section, a special case of trellis shaping, called *sign bit shaping*, is described.

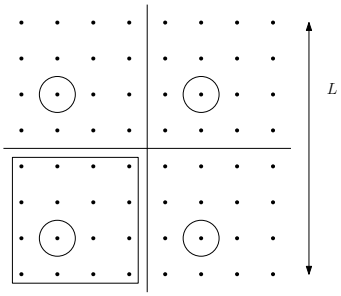

Figure 2. M-ary QAM constellation $\mathcal{A}_M$, illustrated for $M = 64$. Constellation points marked with a circle constitute an equivalence class, while the constellation quadrant marked with a square represents a subset $\mathcal{B}$ of the constellation.

Consider an M-ary QAM constellation, for example $M = 64$ as depicted in Fig. 2. Each constellation point lies in the set $\mathcal{A}_M$, which is the set of all points $x + jy$, where $x, y \in \{\pm 1/2, \pm 3/2, \ldots, \pm(L-1)/2\}$ (thus $M = L^2$). Furthermore, each constellation point is represented by $\log_2 M$ bits as $(\mathbf{z}\ \mathbf{a})$, where $\mathbf{z} = (z_1\ z_2)$ is the vector of *sign bits* and $\mathbf{a}$ is the vector of the *least significant bits* (LSBs). It is possible to define an equivalence class of constellation points which have the same LSBs $\mathbf{a}$ and differ only in their sign bits $\mathbf{z}$. Each point in the class lies in a different quadrant of the constellation depending on the combination of the sign bits as depicted in Fig. 2. Therefore, modifying any of the sign bits of a constellation point implies selecting another point in the equivalence class.

A transmitter implementing the method of sign bit shaping is depicted in Fig. 3. To add the redundancy required for constellation shaping, a convolutional code is considered, which is called the *shaping code* and which we will denote by $\mathcal{C}$. Consider, for example, a binary 4-state rate-$1/2$ linear and time-invariant convolutional code $\mathcal{C}$ with generator matrix

$$\mathbf{G} = \mathbf{G}(D) = [1 + D^2, 1 + D + D^2]$$

where D-transform notation is used. Next define the *syndrome-former* matrix $\mathbf{H}^T = \mathbf{H}^T(D)$ with property

$$\mathbf{G}\mathbf{H}^T = \mathbf{0}.$$

As a consequence, for any codeword $\mathbf{c} = \mathbf{c}(D) \in \mathcal{C}$ we have $\mathbf{c}\mathbf{H}^T = \mathbf{0}$.

For the shaping convolutional code $\mathcal{C}$ described above, a possible syndrome-former matrix $\mathbf{H}^T$ is given by

$$\mathbf{H}^T = [1 + D + D^2, 1 + D^2]^T\ .$$

Consider the trellis shaping scheme depicted in Fig. 3. At time index k, a binary information vector $\mathbf{u}_k$ is divided into two parts: the most significant bit (MSB) s_k and the LSBs $\mathbf{a}_k$. The LSBs $\mathbf{a}_k$ are then mapped via the function $\mathcal{M}(\cdot)$ to a subset $\mathcal{B}$ of $\mathcal{A}_M$ consisting of all constellation points having negative real and imaginary parts (c.f. Fig. 2). The sequence $\mathbf{s} = \mathbf{s}(D)$ is then encoded to produce an output sequence $\mathbf{z} = \mathbf{z}(D)$ via

$$\mathbf{z} = \mathbf{s}(\mathbf{H}^T)^{-1}$$

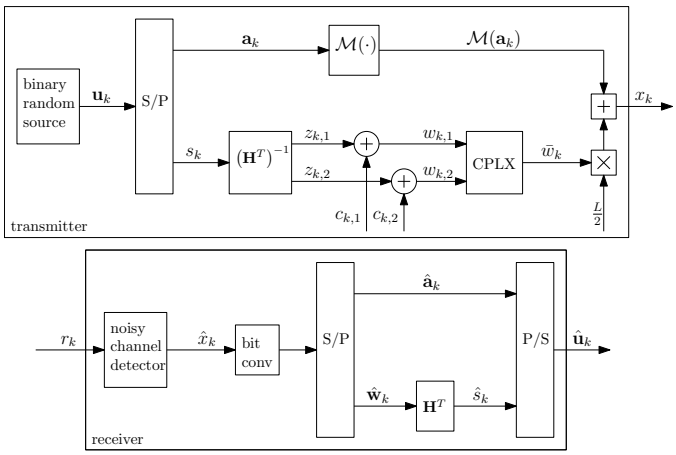

Figure 3. Trellis shaping scheme (sign bit shaping) using a binary 4-state rate-$1/2$ linear time-invariant convolutional code as shaping code.

where $\left(\mathbf{H}^T\right)^{-1}$ is the left-inverse of the syndrome-former matrix. Therefore $\mathbf{s}$ is the syndrome of the output $\mathbf{z}$, whose entry at time index k is $\mathbf{z}_k = (z_{k,1}\ z_{k,2})$. The sign bits $\mathbf{z}_k$ are then processed to determine *modified* sign bits $\mathbf{w}_k = (w_{k,1}\ w_{k,2})$ via $w_{k,i} = (z_{k,i} \oplus c_{k,i})$, where $\mathbf{c}_k = (c_{k,1}\ c_{k,2})$ is the k-th output of the encoder for the shaping convolutional code $\mathcal{C}$ (the modification of the sign bits allows for constellation shaping). Since $\mathbf{c} \in \mathcal{C}$, $\mathbf{w}$ and $\mathbf{z}$ have the same syndrome $\mathbf{s}$. The modified sign bits $\mathbf{w}_k$ are processed to obtain $\bar{w}_k = w_{k,1} + jw_{k,2} \in \mathbb{Z}[j]$, where $\mathbb{Z}[j]$ denotes the set of Gaussian integers.

Trellis shaping is implemented as follows. Consider the trellis diagram of the shaping convolutional code $\mathcal{C}$. Each state S_k corresponds to the contents of the shift-register of the encoder for $\mathcal{C}$, and each state transition corresponds to a possible output $\mathbf{c}_k$ of the encoder of $\mathcal{C}$ and therefore to a constellation point x_k obtained as

$$x_k = \mathcal{M}(\mathbf{a}_k) + \frac{L}{2}\bar{w}_k \tag{1}$$

Considering the trellis diagram at time index k, each transition (trellis branch) from state S_{k-1} to state S_k corresponds to a particular encoder output $\mathbf{c}_k$ and therefore to a corresponding signal point x_k as defined by (1). The branch metric (BM) is defined as

$$BM = |x_k|^2\ .$$

The Viterbi algorithm (VA) [9] searches for the minimum-weight path through the trellis diagram of $\mathcal{C}$ and, as a consequence, the codeword $\mathbf{c}$ allows to transmit the signal $\mathbf{x}$ having minimum energy. A window-based VA is implemented, where in the first window the trellis starts in the all-zero state, and in subsequent windows the start state is set to equal the final state of the previous window (it is important that the transmitted sequence corresponds to a valid codeword $\mathbf{c} \in \mathcal{C}$).

At the receiver, a conventional constellation detector forms an estimate $\hat{x}_k$ of each transmitted symbol x_k, which is then bit demapped. The resulting bits are divided into two parts: the

estimated LSBs $\hat{\mathbf{a}}_k$ and the estimated modified sign bits $\hat{\mathbf{w}}_k$. The estimate $\hat{\mathbf{w}}$ is processed to obtain the estimated syndrome

$$\hat{\mathbf{s}} = \hat{\mathbf{w}}\mathbf{H}^T \ .$$

The estimated information vector $\hat{\mathbf{u}}_k$ is obtained by combining the estimated LSBs $\hat{\mathbf{a}}_k$ and the estimated syndrome $\hat{\mathbf{s}}_k$.

III. Proposed System Description

This section describes the system model for the proposed scheme. In the following description, we specify the processing performed by each node in turn.

A. Transmitter at User Nodes

Each user node $N^{(i)}$, where $i \in \{1, 2\}$, applies sign bit shaping for transmission as depicted in Fig. 3 (we use the same notation for variables as in this figure, but with an additional superscript i to specify the user). At time index k, user node $N^{(i)}$ divides its binary information sequence $\mathbf{u}_k^{(i)}$ into two parts: the MSB $s_k^{(i)}$ and LSBs $\mathbf{a}_k^{(i)}$. Each bit in the syndrome sequence $\mathbf{s}^{(i)}$ is encoded as described in Section II, yielding the sign bits $\mathbf{z}_k^{(i)}$. The sign bit sequence is then further processed by adding (modulo-2) the k-th output $\mathbf{c}_k^{(i)}$ of the encoder of $\mathcal{C}$ for user node $N^{(i)}$. The codeword $\mathbf{c}^{(i)} \in \mathcal{C}$ effects constellation shaping, and it is obtained using trellis shaping as described in Section II. The modified sign bits $\mathbf{w}_k^{(i)}$ and the LSBs $\mathbf{a}_k^{(i)}$ are then combined, yielding the transmitted signal $x_k^{(i)} \in \mathcal{A}_M$ which, according to (1), can be expressed as

$$x_k^{(i)} = \mathcal{M}\big(\mathbf{a}_k^{(i)}\big) + \frac{L}{2}\bar{w}_k^{(i)} \ . \tag{2}$$

In the MA phase, each user node $N^{(i)}$ *simultaneously* transmits its modulated signal $x_k^{(i)}$ ($i \in \{1, 2\}$).

B. Processing at Relay Node

At time index k, the relay node receives the superimposed signal

$$r_k^{(R)} = x_k^{(sum)} + n_k^{(R)}$$

where $n_k^{(R)}$ is a zero-mean complex Gaussian random variable with variance σ_R^2 and $x_k^{(sum)} = x_k^{(1)} + x_k^{(2)}$. Note that $x_k^{sum} \in \mathcal{A}_{sum}$, where the "sum-constellation" $\mathcal{A}_{sum}$ is the set of all points $x + jy$ where $x, y \in \{0, \pm 1, \pm 2, \ldots, \pm(L-1)\}$. The relay has the purpose of recovering $x_k^{(sum)}$ from the received signal and broadcasting a network-coded signal suitable for each user node to extract the information vector of the other user. To recover $x_k^{(sum)}$, the received noisy signal $r_k^{(R)}$ is input to a conventional minimum-distance detector [10] operating on the sum-constellation, yielding the signal $\hat{x}_k^{(sum)}$. Consider, for ease of exposition, correct detection of the superimposed signal, i.e., $\hat{x}_k^{(sum)} = x_k^{(sum)}$. A first approach to relaying consists in simply broadcasting this signal, as each user node can extract the information of the other user. For example, if user node $N^{(2)}$ receives $x_k^{(sum)}$, then by subtracting its own signal $x_k^{(2)}$ it can easily recover $x_k^{(1)}$ and apply the simple bit demapping and syndrome-former operations as shown in the lower part of Fig. 3.

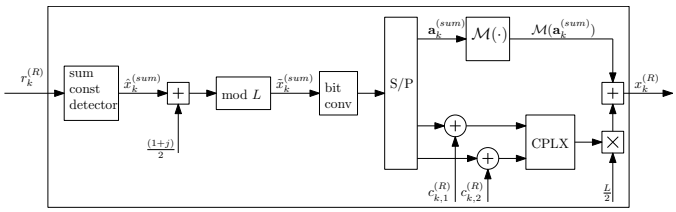

Figure 4. Relay node scheme.

A second approach to relaying, which has the ability to reduce the transmitted energy in the BC phase, is to transmit as network-coded signal a point which lies in the original constellation $\mathcal{A}_M$. After the detection of $x_k^{(sum)}$, a shift of $\frac{(1+j)}{2}$ is required to compensate the bias between the two constellations $\mathcal{A}_{sum}$ and $\mathcal{A}_M$. This is followed by a modulo-L operation[1] which is applied per dimension. As a result, the transmitted signal at the relay is

$$\tilde{x}_k^{(sum)} = x_k^{(sum)} + \frac{(1+j)}{2} + L\bar{p}_k \tag{3}$$

where $\bar{p}_k \in \mathbb{Z}[j]$ is due to the modulo-L operation, and its value is fixed by the fact that $\tilde{x}_k^{(sum)} \in \mathcal{A}_M$. To see that this signal is sufficient for broadcast, consider for example user node $N^{(2)}$, which receives a noisy version of $\tilde{x}_k^{(sum)}$; in case of correct detection of $\tilde{x}_k^{(sum)}$, it may be easily seen that the subtraction of the local signal $x_k^{(2)}$ and of the shift value $\frac{(1+j)}{2}$, and a modulo-L operation allow correct extraction of the signal $x_k^{(1)}$.

A third approach is to apply the principle of trellis shaping also at the relay node; the signal processing required is depicted in Fig. 4. In this case, the transmission in the BC phase may be made more energy efficient by applying constellation shaping also at the relay. Here, the shaping convolutional code $\mathcal{C}$ applied at the relay is the same as that applied at the user nodes.

Consider, for simplicity, correct detection of the superimposed signal $x_k^{(sum)}$, which is then processed via (3) to obtain $\tilde{x}_k^{(sum)}$. After bit demapping, the sign bits are further modified by an XOR operation with the k-th output $\mathbf{c}_k^{(R)} = (c_{k,1}^{(R)}\ c_{k,2}^{(R)})$ of the relay's encoder for the shaping code $\mathcal{C}$. The signal $x_k^{(R)} \in \mathcal{A}_M$ broadcast by the relay node may be expressed as

$$x_k^{(R)} = \tilde{x}_k^{(sum)} + \frac{L}{2}\bar{c}_k^{(R)} + L\bar{g}_k \tag{4}$$

where $\bar{c}_k^{(R)} = c_{k,1}^{(R)} + jc_{k,2}^{(R)} \in \mathbb{Z}[j]$ corresponds to the k-th output of the encoder of $\mathcal{C}$, and $\bar{g}_k \in \mathbb{Z}[j]$ ensures that the signal transmitted at the relay lies in $\mathcal{A}_M$.

Fig. 5 provides a comparison for $M = 64$ of the transmitted signal's energy in the BC phase using the three relaying approaches described above. At the top of Fig. 5, the distribution

[1]Throughout this paper, the phrase "modulo-L" is used to mean reduction modulo-L to the constellation $\mathcal{A}_M$.

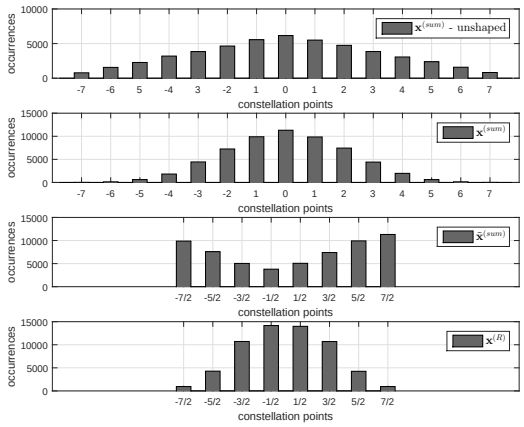

Figure 5. Distribution (per dimension) of transmitted signal at the relay using 64-QAM. Top to bottom: BC of $\mathbf{x}^{(sum)}$ with no shaping at user nodes; BC of $\mathbf{x}^{(sum)}$ with trellis shaping at user nodes; BC of $\tilde{\mathbf{x}}^{(sum)}$ as given by (3); BC of $\mathbf{x}^{(R)}$ as given by (4).

of BC signal energy for the case of an unshaped PNC system is also depicted as a reference. It may be noticed that even when no shaping is implemented at the user nodes, signal superposition naturally induces a basic form of "triangular" constellation shaping. The second histogram in Fig. 5 is that for the transmitted signal $\mathbf{x}^{(sum)}$ at the relay when trellis shaping is implemented at each user node's transmitter. As expected, the distribution of the BC signal is better shaped as compared to the case where no shaping is employed by the users (note that the sum of two Gaussian distributions yields a Gaussian distribution). The third histogram corresponds to the signal $\tilde{\mathbf{x}}^{(sum)}$ as given by (3). The modulo-L operation allows the relay to transmit a signal in $\mathcal{A}_M$, and as a consequence the energy transmitted is reduced compared to the previous two cases. On the other hand, the modulo-L operation does not provide a near-Gaussian distribution of the BC signal. In the final histogram in Fig. 5, the signal transmitted from the relay in the proposed scheme $\mathbf{x}^{(R)}$ is depicted. Trellis shaping at the relay allows to re-introduce constellation shaping after the modulo-L operation, and as a result the distribution of the signal is both near-Gaussian and lying in the original constellation $\mathcal{A}_M$.

C. Receiver at User Nodes

In this subsection, we assume the use of the most energy-efficient scheme, i.e., the use of trellis shaping at the relay as described in the previous subsection. Consider without loss of generality the receiver for user node $N^{(2)}$; this is depicted in Fig. 6. User node 2 receives at time index k the noisy signal

$$r_k^{(2)} = x_k^{(R)} + n_k^{(2)}$$

where $n_k^{(2)} \sim \mathcal{CN}(0, \sigma^2_{N^{(2)}})$. To detect the estimated signal $\hat{x}_k^{(R)}$, a conventional minimum distance detector is used. To extract the information from $x_k^{(R)}$, the local signal $x_k^{(2)}$ and the shift value $\frac{(1+j)}{2}$ are subtracted. Assuming correct detection

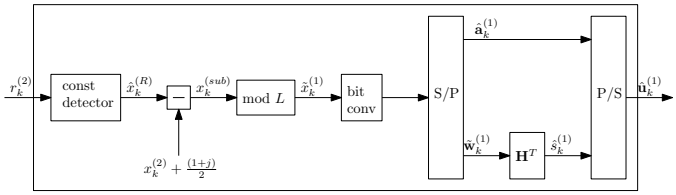

Figure 6. Receiver processing for user node 2. Analogous operations are implemented at the receiver for user node 1.

of the relay signal $x_k^{(R)}$, the extracted signal can be written as (recalling (2), (3) and (4))

$$\begin{aligned} x_k^{(sub)} &= x_k^{(1)} + \frac{L}{2}\bar{c}_k^{(R)} + L(\bar{g}_k + \bar{p}_k) \\ &= \mathcal{M}\big(\mathbf{a}_k^{(1)}\big) + \frac{L}{2}\big(\bar{w}_k^{(1)} + \bar{c}_k^{(R)}\big) + L\big(\bar{g}_k + \bar{p}_k\big) \end{aligned} \tag{5}$$

Note that neglecting the last of the three additive terms in (5) yields a point in $\mathcal{A}_M$ in all cases *except* the case where $w_{k,j}^{(1)} = c_{k,j}^{(R)} = 1$ for some $j \in \{1, 2\}$. However, in that case, $\frac{L}{2}(w_{k,j}^{(1)} + c_{k,j}^{(R)}) = L$. It follows that after the modulo-L operation we have

$$\tilde{x}_k^{(1)} = \mathcal{M}\big(\mathbf{a}_k^{(1)}\big) + \frac{L}{2}\big(\bar{w}_k^{(1)} \oplus \bar{c}_k^{(R)}\big)$$

where $\bar{w}_k^{(1)} \oplus \bar{c}_k^{(R)} = (w_{k,1}^{(1)} \oplus c_{k,1}^{(R)}) + j(w_{k,2}^{(1)} \oplus c_{k,2}^{(R)})$. After bit demapping, the corresponding sequence is divided into two parts: the modified sign bits $\tilde{\mathbf{w}}_k^{(1)} = \big(\mathbf{w}_k^{(1)} \oplus \mathbf{c}_k^{(R)}\big)$ and the LSBs $\mathbf{a}_k^{(1)}$. As described in Section II, using the same shaping code $\mathcal{C}$ at user nodes and at the relay, the modified sign bit sequence $\tilde{\mathbf{w}}^{(1)}$ has the same syndrome as $\mathbf{w}^{(1)}$; therefore the syndrome $\mathbf{s}^{(1)}$ can be extracted. $\mathbf{a}_k^{(1)}$ and $s_k^{(1)}$ are then combined to obtain the binary information vector $\mathbf{u}_k^{(1)}$. User node $N^{(1)}$ extracts $\mathbf{u}_k^{(2)}$ from $x_k^{(R)}$ in a similar manner.

IV. Simulation Results

This section presents simulated performance results for the system described in Section III with simulation parameters given in the following.

A M-ary QAM format is considered for all transmissions. In particular, the cases $M \in \{16, 64, 256\}$ are simulated. All links are assumed to be AWGN channels. The results show the BER performance of the system using the three relaying approaches described in Section III, considering a window-size of 20 for the VA. Furthermore, the unshaped PNC system is used as a reference. The signal-to-noise ratio (SNR) for the shaped PNC system in the MA phase is defined as $\text{SNR} = \frac{1}{R}\frac{E[|\mathbf{x}^{(i)}|^2]}{\sigma^2_R}$, where $R = 1 - \frac{1}{\log_2 M}$ is the rate of the shaping code and $E[|\mathbf{x}^{(i)}|^2]/R$ therefore represents the average transmitted energy per information bit. For unshaped PNC, we have $\text{SNR} = \frac{E[|\mathbf{x}^{(i)}|^2]}{\sigma^2_R}$. Similarly in the BC phase, the SNR for shaped PNC is $\text{SNR} = \frac{1}{R}\frac{E[|\mathbf{x}^{(R)}|^2]}{\sigma^2_{N^{(i)}}}$ while for unshaped PNC the rate factor R is not considered. The simulations assume an equal SNR in the MA phase and the BC phase.

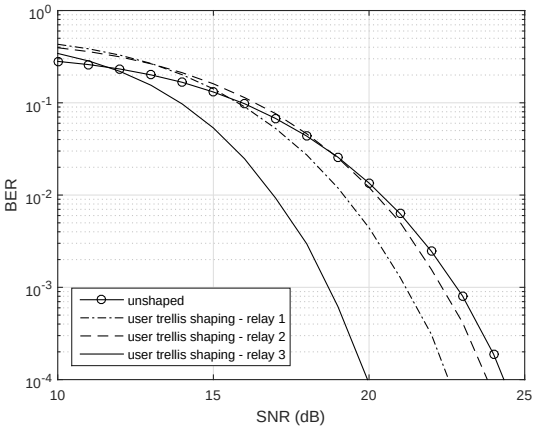

Figure 7. End-to-end BER for the case of 16-QAM. PNC with trellis shaping at the user nodes and the first approach at the relay (relay 1; dash-dotted line) shows a gain of 1.5dB compared with unshaped PNC. The proposed PNC with trellis shaping at both user and relay nodes (relay 3; solid line) has a gain of 3.9dB.

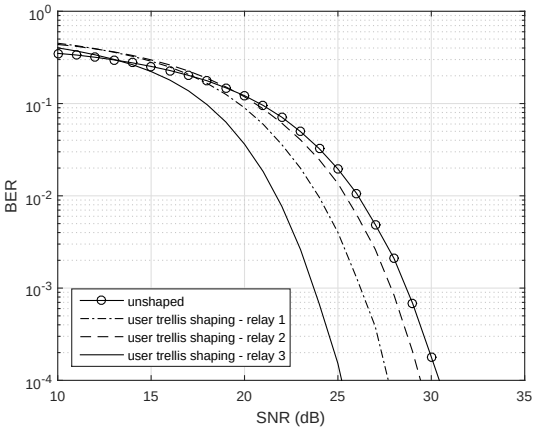

Figure 8. End-to-end BER for the case of 64-QAM. PNC with trellis shaping at the user nodes and the first approach at the relay (relay 1; dash-dotted line) shows a gain of 2.4dB compared with unshaped PNC. The proposed PNC with trellis shaping at both user and relay nodes (relay 3; solid line) has a gain of 5dB.

In Figs. 7-9 the simulated end-to-end BER for 16, 64, and 256-QAM are shown respectively. The proposed scheme with trellis shaping at the relay achieves a gain of 5.3dB compared to the unshaped PNC in case of 256-QAM. The results also report the BER performance of a scheme in which trellis shaping is implemented only at the user nodes and the first relaying approach is considered. This scheme, in the case of 256-QAM, shows a gain of 2.8dB compared to the unshaped PNC. Both approaches have improved performances compared to the unshaped PNC in all of the M-QAM cases simulated. The second approach at the relay has performance close to unshaped PNC. This is due to the effect of the modulo-L operation on the distribution of the signal transmitted at the relay.

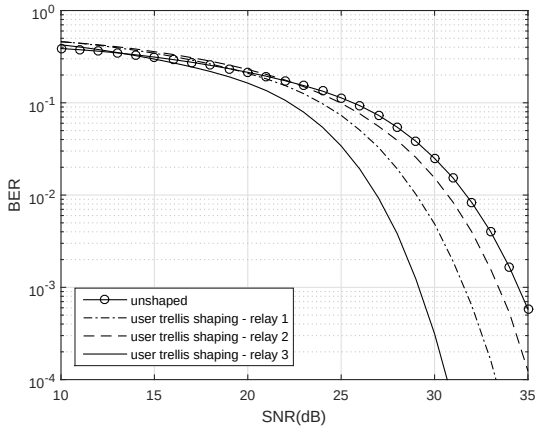

Figure 9. End-to-end BER for the case of 256-QAM. PNC with trellis shaping at the user nodes and the first approach at the relay (relay 1; dash-dotted line) shows a gain of 2.8dB compared with unshaped PNC. The proposed PNC with trellis shaping at both user and relay nodes (relay 3; solid line) has a gain of 5.3dB.

V. Conclusion

In this paper we have proposed a new trellis shaping approach with application to a PNC system using M-ary QAM over the TWRC. In the proposed scheme, trellis shaping is implemented in both MA and BC phases in order to minimize the average energy in the end-to-end communication. Simulation results show that the proposed scheme provides a significantly increased performance in terms of the achievable BER, with 5.3dB shaping gain available at a BER of 10^{-3} in the case of 256-QAM signaling. Future work will investigate the use of channel coding both at the users and at the relay for the proposed system.

References

[1] S. C. Liew, S. Zhang, and L. Lu, "Physical-layer network coding : Tutorial, survey, and beyond," *Physical Commun.*, vol. 6, pp. 4–42, Mar 2013.

[2] S. Zhang, S. C. Liew, and P. P. Lam, "Hot topic: Physical-layer network coding," in *ACM MobiCom '06*, Sep. 2006, pp. 358–365.

[3] S. Pfletschinger, "A practical physical-layer network coding scheme for the uplink of the two-way relay channel," in *ASILOMAR*, Nov. 2011, pp. 1997–2001.

[4] R. Y. Chang, S. J. Lin, and W. H. Chung, "Symbol and bit mapping optimization for physical-layer network coding with pulse amplitude modulation," *IEEE Transactions on Wireless Communications*, vol. 12, no. 8, pp. 3956–3967, Aug. 2013.

[5] S. Wang, Q. Song, L. Guo, and A. Jamalipour, "Constellation mapping for physical-layer network coding with M-QAM modulation," in *GLOBECOM'12*, Dec. 2012, pp. 4429–4434.

[6] A. R. Calderbank and L. H. Ozarow, "Nonequiprobable signaling on the Gaussian channel," *IEEE Trans. Inf. Theory*, vol. 36, no. 4, pp. 726–740, Jul. 1990.

[7] Y. Hou, Z. Chen, B. Xia, and H. Liu, "Physical-layer shaped network coding with M-PAM modulation," in *GLOBECOM '14*, Dec. 2014, pp. 1571–1576.

[8] G. D. Forney, "Trellis shaping," *IEEE Trans. Inf. Theory*, vol. 38, no. 2, pp. 281–300, Mar. 1992.

[9] ——, "The Viterbi algorithm," *Proc. IEEE*, vol. 61, no. 3, pp. 268–278, Mar. 1973.

[10] J. Proakis and M. Salehi, *Communication Systems Engineering*. Prentice Hall, 1994.